EECS C145B / BioE C165: Image Processing and Reconstruction Tomography

Lecture 15

Jonathan S. Maltz

jon@eecs.berkeley.edu
http://muti.lbl.gov/145b
510-486-6744

Topics covered

1. Encoding position in MRI
2. Frequency encoding
3. Projection MRI
4. Phase encoding
5. Slice selection
6. The spin warp sequence
7. Mathematical basis of joint frequency and phase encoding (2D FT MRI)
8. MRI frontiers: high field human imaging
9. MRI frontiers: diffusion tensor imaging
10. Comparison of MRI, x-ray CT and ECT.

Reading

Assigned reading (several views of same material):

- MRI - the basics pp. 67-81. 88-113, 137-159 (in Course Reader).
- Course Reader, pp. 462-468.
- Webb, "The Physics of Medical Imaging", Institute of Physics Publishing (1998), pp. 412-487 (in Course Reader)
- MRI Primer pp. 96-115 (in Course Reader).

Additional reading:

- Cho, "Foundations of Medical Imaging", John Wiley and Sons (1993), Chapters 9 and 10.

Encoding position in MRI

- At this point, we have learned how to obtain contrast between tissues having different chemical and physical properties. However, we cannot identify **where** these tissues are within the field of view.
- By adding spatial encoding information, MR spectroscopy becomes MR imaging.
- Spatial information is encoded using **gradient fields** that have components along the x, y and z axes. These gradients are usually **linear ramps**.
- When a magnetic field gradient along the x-axis, G_x, is applied, the Larmor frequency of a nucleus becomes proportional to its x-position:

$$\omega(x) = \gamma(B_0 + xG_x)$$

Encoding position in MRI

- Thus, if we apply the Fourier transform (or, because of duality, its inverse) to the sum of the FIDs that is present in the **received RF signal** at the RF coil, we will find spectral peaks in the magnitude spectrum whose **height** is proportional to the **number of resonant protons along each line of equal x position**. This spectrum will thus be the **line integral** of the imaged distribution $f(x, y)$ at the angle $\theta = 0$.
- We identify this as the **Radon projection** of $f(x, y)$, $p_{\boldsymbol{\theta}}(s)$.

Given this fact, how can we manipulate the gradient field in the x-y plane so that we have sufficient data to reconstruct the image?

Spatial encoding: frequency encoding

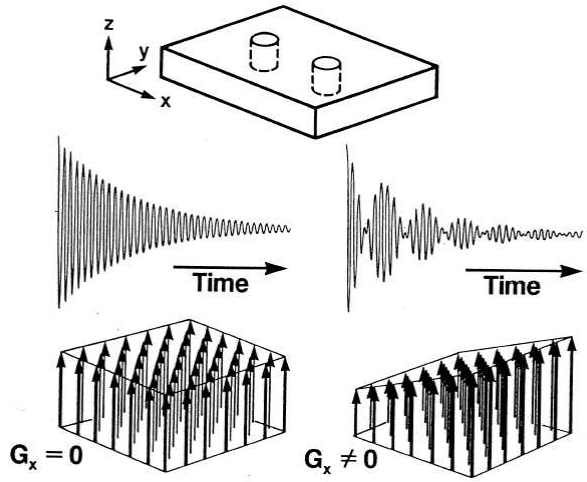

Figure 1.10 ▪ In the presence of a field gradient, two tubes of water will have Larmor frequencies that depend on their spatial position. The Fourier transform of their FID is the projection onto the axes of the field gradient.

Source: Shaw p. 12

Spatial encoding example

0	1	1
1	2	0
-2	0	1

Source: Hashemi p. 100

Assume that we have chosen TE and TR to achieve a **specific contrast**. Then the image we reconstruct will have greyscale intensity values based on this contrast. The figure above defines a true spatial contrast distribution $\rho(x, y)$ that we must reconstruct from NMR FID signals. $\rho(x, y)$ is called the **weighted spin density**. It depends on the local T_1, T_2 and proton spin density.

Spatial encoding example

0	cosωot	cosωot
cosωot	2cosωot	0
-2cosωot	0	cosωot

→ 4 cosωot

Figure 11-4. Each pixel is also assigned a frequency ω_0, and represented as A cos ω_0t, where A is the magnitude.

Source: Hashemi p. 100

When B_0 is applied, in the absence of a gradient field, the sinusoidal components of the FID contributions of each region after a 90 degree pulse will all have the **same Larmor frequency** ω_0, and the **same phase**. The FID received at the RF coil will thus simply be a sinusoid whose amplitude is the sum of the amplitudes of all the 9 regions (multiplied by an exponentially decaying envelope).

Spatial encoding example: application of G_x

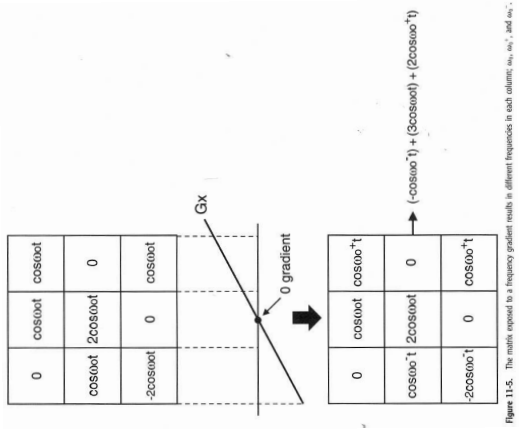

Source: Hashemi p. 101

After G_x is applied, the central column of regions contains nuclei that **continue to precess** at w_0 since they experience **no change in field** with the addition of the gradient. However, the nuclei in the **left column** precess at a **lower frequency** ω_0^- and those in the **right column** at a **higher frequency** ω_0^+.

Spatial encoding example: application of G_x

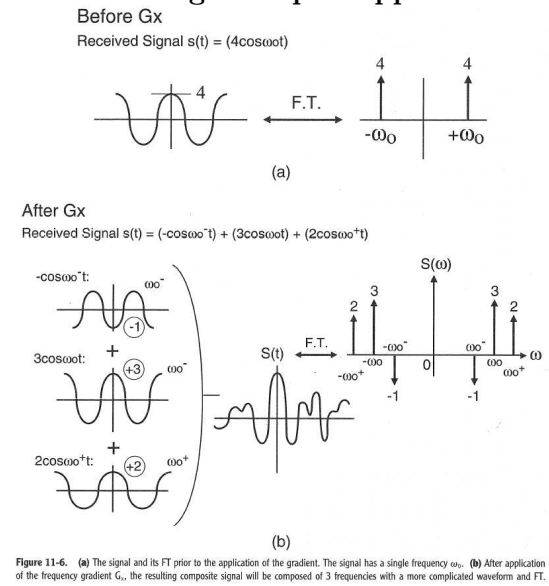

Figure 11-6. **(a)** The signal and its FT prior to the application of the gradient. The signal has a single frequency ω_0. **(b)** After application of the frequency gradient G_x, the resulting composite signal will be composed of 3 frequencies with a more complicated waveform and FT.

Source: Hashemi p. 102

Spatial encoding example: application of G_x

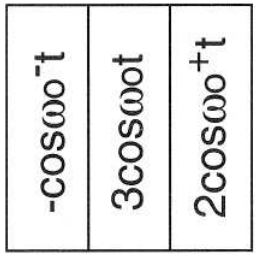

Figure 11-7. The sum of the signals in each column. Since the signals belonging to the same column have the same frequency, they are additive.

Source: Hashemi p. 103

In the continuous case, the magnitude Fourier spectrum of the received FID gives the Radon projection for rays travelling along the columns of the distribution. The radial parameter of the Radon transform s is thus given by:

$$s = \frac{\omega_0 - \gamma B_0}{\gamma G_\theta}$$

where $G_\theta = G_x$ is the magnitude of the resultant gradient vector oriented along $\boldsymbol{\theta}$. In this case $\theta = 0$.

Projection MRI

- MRI scanners have a **second adjustable gradient field** along the y-axis, G_y.
- When we simultaneously apply G_x and G_y, we get a **resultant field** in the x-y plane that has magnitude:

$$|\mathbf{G}_\theta| = G_x \cos(\theta) + G_y \sin(\theta)$$

and direction:

$$\angle \mathbf{G}_{xy} = \arctan \theta$$

- To obtain the projection $p_{\boldsymbol{\theta}}(s)$, we need only adjust G_x and G_y so that the resultant field is oriented along $\boldsymbol{\theta}$.
- To obtain I **angular projections**, we must apply I **pulse sequences**, each having a **different set** of G_x and G_y values.
- Image reconstruction can be performed using **any algorithm that can numerically invert the Radon transform**, such as those suitable for x-ray CT reconstruction.

Projection MRI imaging: pulse sequence

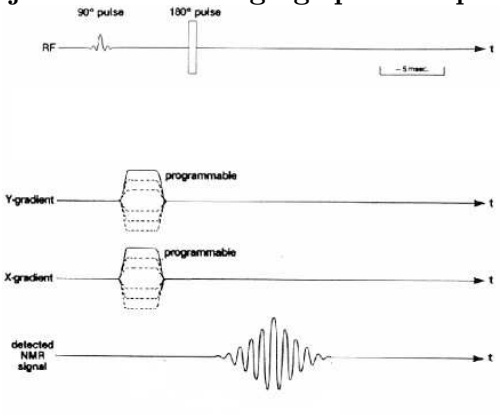

Source: Shaw p. 23 (modified)

By adjusting the x and y gradients, the resultant gradient field can be oriented along any vector $\boldsymbol{\theta}$. The magnitude FT of the resulting RF signal gives the line integrals perpendicular to $\boldsymbol{\theta}$. This pulse sequence must be repeated for each projection acquired using different combinations of G_x and G_y.

Projection MRI imaging: pulse sequence

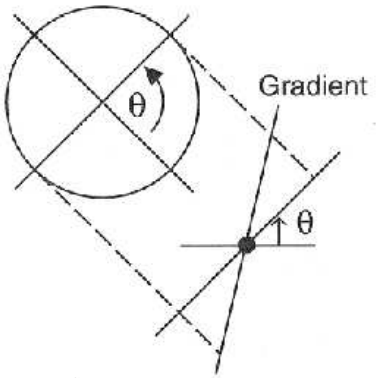

Source: Hashemi p. 103

Rotating the gradient field so that it is oriented along $\boldsymbol{\theta}$ gives the Radon projection $p_{\boldsymbol{\theta}}(s)$.

Projection MRI and phase encoding

- Projection MRI allows us to reconstruct x and y position using the inverse Radon transform. Projection MRI is **seldom used** in practice because it is **very sensitive to inhomogenities in the applied magnetic fields B_0 and the gradient field.**
- Most MRI studies employ pulse sequences rely on **phase encoding** to encode spatial position along the y-axis.
- The basis of phase encoding is to **manipulate the gradient fields** G_x and G_y in such a way that the magnitude of the FT gives the x-position and the phase gives the y-position. Combining frequency and phase encoding is a method of **sampling the 2D Fourier plane**. This is equivalent to sampling the MRI real space weighted spin density $\rho(x, y)$.

Spatial encoding: phase encoding example

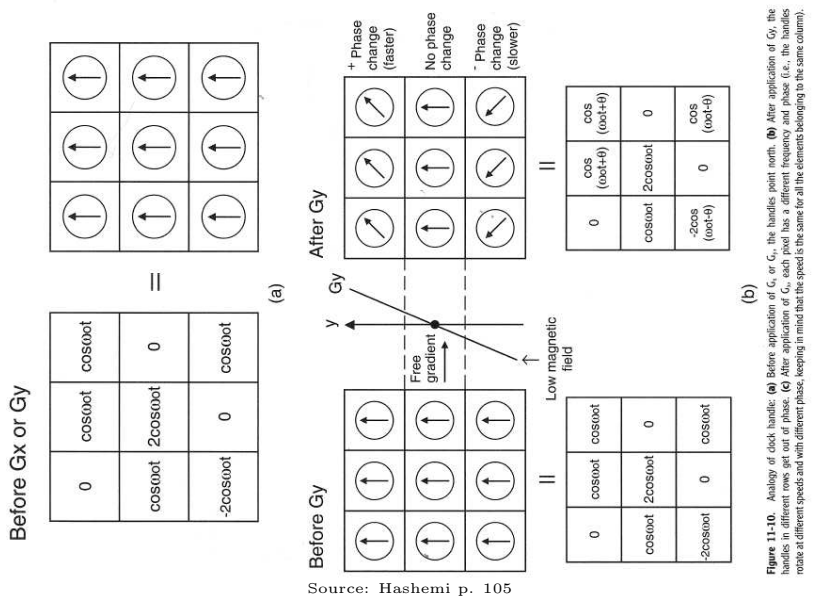

Figure 11-10. Analogy of clock handles: **(a)** Before application of G_x or G_y, the handles point north. **(b)** After application of G_y, the handles in different rows get out of phase. **(c)** After application of G_x, each pixel has a different frequency and phase (i.e., the handles rotate at different speeds and with different phase; keeping in mind that the speed is the same for all the elements belonging to the same column).

Source: Hashemi p. 105

Spatial encoding: phase encoding example

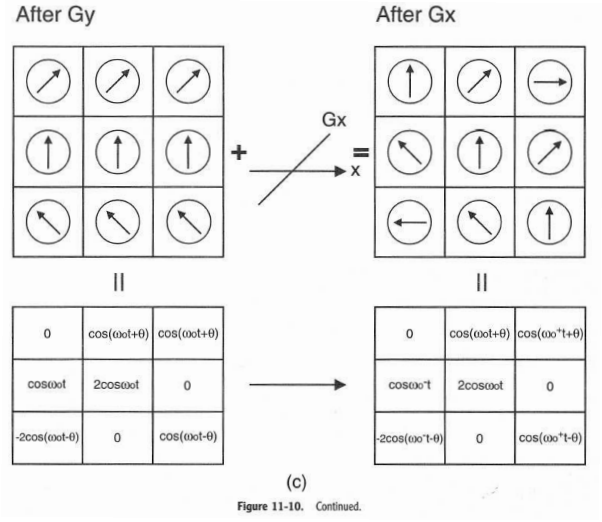

Source: Hashemi p. 106

After application of G_x and G_y, different regions have unique frequency and phase parameter pairs.

Spatial encoding: z-slice selection

- Before we discuss the pulse sequences used to perform spatial and phase encoding on a single transaxial slice, we will first examine the process of **selecting the transaxial slice to be imaged.**
- Conventionally, as in x-ray CT and ECT, we image a 3D distrubution **slice-by-slic**e.
- Slice selection is achieved by **frequency encoding** along the z-axis using a **third gradient field** G_z.
- An RF pulse is applied in the presence of G_z that contains frequency components that are the **Larmor frequencies of nuclei at a specific z value**.
- The **wider the bandwidth** of this pulse, the **thicker** is the slice and the **lower the resolution** along the z-axis.
- For a pulse of given bandwidth, the **steeper** the gradient field, the **thinner** the slice and the **higher** the resolution along the z-axis.

Spatial encoding: z-slice selection

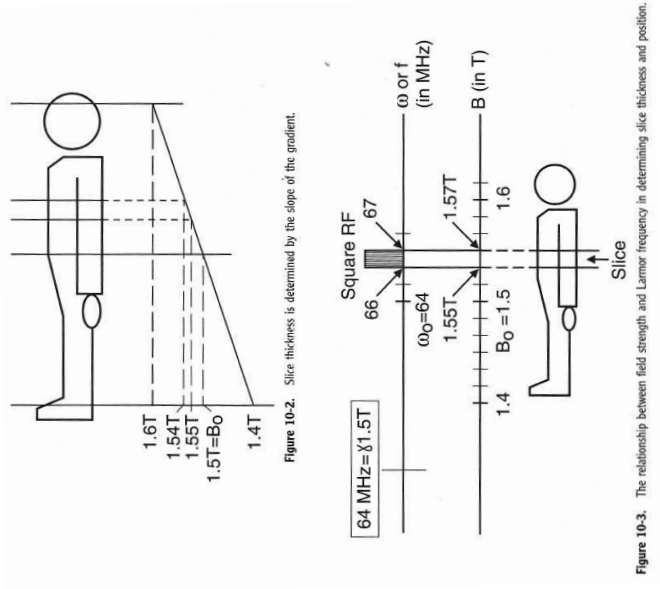

Source: Hashemi p. 89

Spatial encoding: z-slice selection

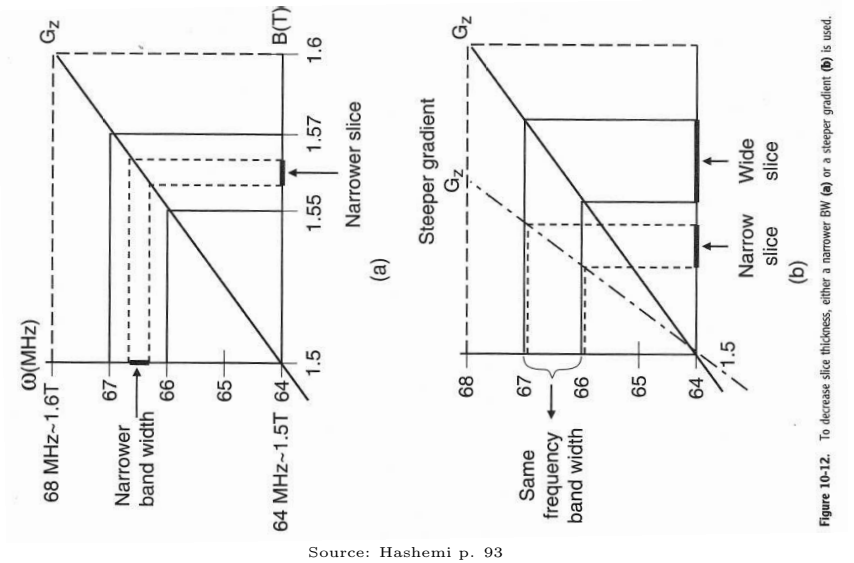

Source: Hashemi p. 93

Spatial encoding: the spin-warp pulse sequence

We now study a **practical** imaging pulse/gradient protocol that employs **both frequency and phase encoding** that uses the **spin-warp** sequence. This protocol proceeds as follows:

1. With the z-gradient applied, a narrow band 90 degree RF pulse **selects the transaxial slice** to be imaged.
2. The applied field G_z is inverted. This **time reversal gradient** has a similar effect to a 180 degree pulse and undoes the unwanted dephasing caused by the z-gradient.
3. Phase information is encoded via the application of G_y. Nuclei along **lines of constant** y experience **equal phase shift**.

Spatial encoding: the spin-warp pulse sequence

4. The **frequency encoding (or readout)** gradient G_x is applied.
   - To avoid **unwanted signal decay** during the interval between the shutting off of G_y and the rising edge of G_x, an x **time-reversal gradient** is applied while phase encoding is taking place. An echo-like FID results when rephasing occurs.
   - This **gradient echo** occurs at a time well separated from the noisy switching transients associated with the gradient fields being turned on and off.
   - To increase SNR further, a **180 degree pulse** can be included that removes the dephasing effects of **field inhomogeneities.**
   - The x time-reversal gradient must be **inverted** in this case, and the **gradient echo must coincide with the spin echo** that is due to the 180 degree pulse. Chemical shift artifacts result if this is not the case.

Spatial encoding: the spin-warp pulse sequence

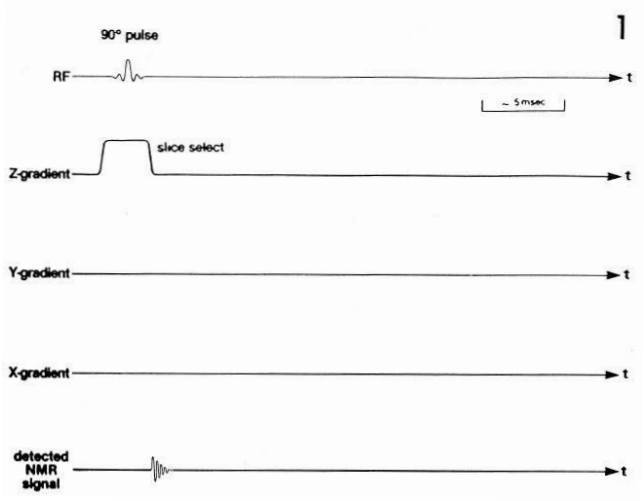

Source: Shaw p. 19

Application of a 90 degree pulse in the presence of G_z excites a transaxial slice whose nuclei have Larmor frequencies within the pulse bandwidth.

Spatial encoding: the spin-warp pulse sequence

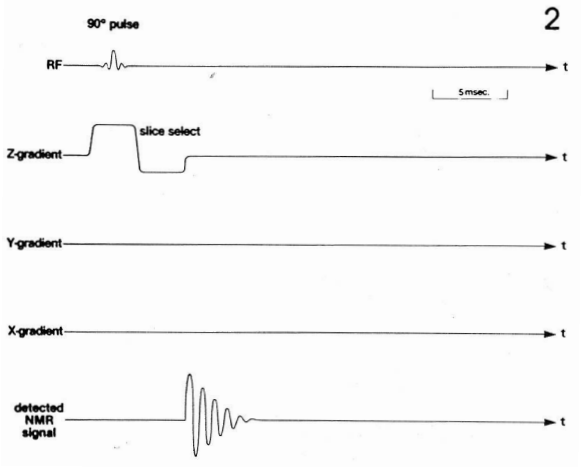

Source: Shaw p. 19

Inverting the slope of G_z following its inital application removes unwanted dephasing in the x-y plane caused by the gradient field. This is called a time-reversal z-gradient. A larger FID results as a consequence.

Spatial encoding: the spin-warp pulse sequence

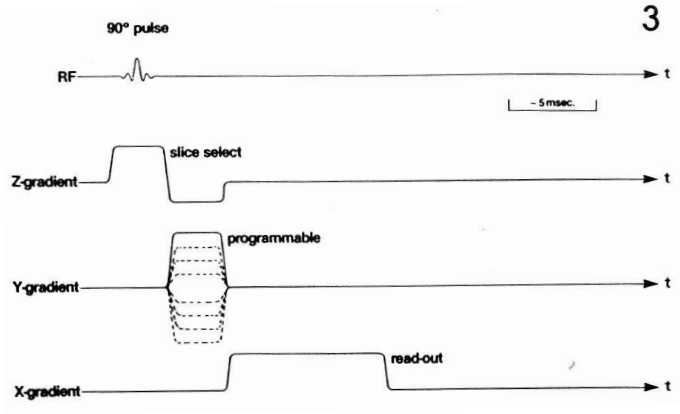

Source: Shaw p. 20

Application of G_y causes phase changes in the nuclear spins that are proportional to y-position. Subsequent application of G_x frequency encodes the x-position of the nuclei.

Spatial encoding: the spin-warp pulse sequence

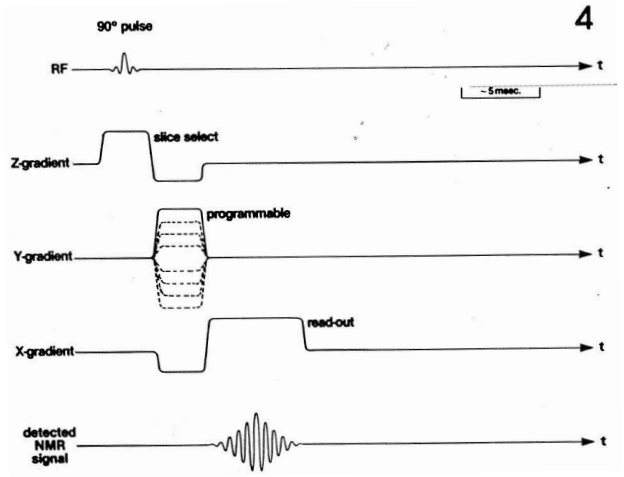

Source: Shaw p. 20

Modification of the sequence through the inclusion of a time-reversal x-gradient removes dephasing through spin reversal. An echo-like FID is produced.

Spatial encoding: the spin-warp pulse sequence

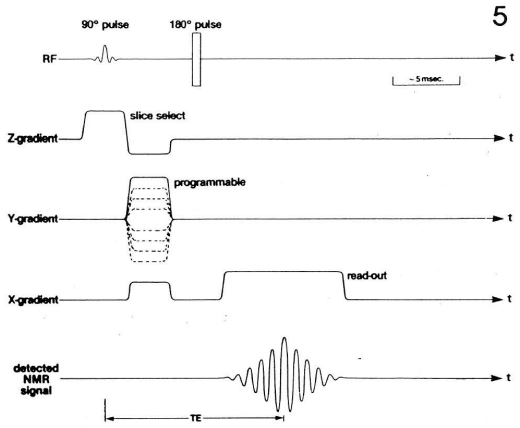

Source: Shaw p. 20

The sequence can be further improved by incorporating a 180 degree pulse to undo dephasing caused by magnet inhomogeneities. The time-reversal x-gradient therefore needs to be inverted to obtain the same effect as it had in the previous sequence. The gradient and spin echoes must coincide to avoid artifacts.

The mathematical basis of 2D Fourier transform imaging

- Imaging that proceeds according to the above protocol is called **2D Fourier transform imaging**, as it involves **sampling** the 2D Fourier transform plane.
- For each desired row of image pixels (y-value), we need to perform a spin-warp pulse sequence.
- Each time we do this, we employ a different value of G_y.
- To really understand how phase encoding works and consequently, how to reconstruct an image, we now study the mathematical description of 2D FT MR imaging.

The mathematical basis of 2D Fourier transform imaging

- We know that the RF coil signal is proportional to the transverse plane magnetisation M_{xy}. In the presence of a linear gradient, this is given by the Bloch equation:

$$\frac{dM_{xy}}{dt} = \left(\jmath\,\omega_0 - \frac{1}{T_2} - \jmath\,\gamma\,B_g(\mathbf{r}) \right) M_{xy}$$

where $M_{xy} = M_y + jM_x$, and $B_g(\mathbf{r})$ is magnitude of the gradient field at a point $\mathbf{r}$:

$$\begin{aligned} B_g(\mathbf{r}) &= (x\,\mathbf{e}_x + y\,\mathbf{e}_y + z\,\mathbf{e}_z) \cdot \Big[G_x(t)\,\mathbf{e}_x + G_y(t)\,\mathbf{e}_y + G_z(t)\,\mathbf{e}_z \Big] \\ &= \mathbf{r} \cdot \mathbf{G}(t). \end{aligned}$$

where $\mathbf{e}_x$, $\mathbf{e}_y$ and $\mathbf{e}_z$ are unit vectors along the x, y and z axes, respectively.

The mathematical basis of 2D Fourier transform imaging

- The solution to the above Bloch equation is:

$$M_{xy}(\mathbf{r}, t) = M_0\,\rho(\mathbf{r})\,\mathrm{e}^{\,-\jmath\gamma\mathbf{r}\cdot\int_0^t \mathbf{G}(\tau)\,d\tau}$$

where M_0 is the magnetisation at thermal equilibrium (before any RF pulse was applied) and $\rho(\mathbf{r})$ is the contrast-weighted spin density (which depends on T_1, T_2 and the proton spin density ρ_0 at location $\mathbf{r}$).

- This solution represents the **single FID** produced by a nucleus "singing" at position $\mathbf{r}$.
- The T_2-dependent decaying FID envelope is absorbed into the factor $\rho(\mathbf{r})$.
- The exponential factor is the **sinusoidal component**, whose frequency and phase **at time t at location $\mathbf{r}$** are determined by the **cumulative effects of the gradient fields** applied up until time t.

The mathematical basis of 2D Fourier transform imaging

- In MRI, we cannot individually sample the $M_{xy}(\mathbf{r}, t)$, since each is a measurement at a **single point** at a certain time. What we measure is the **sum** of all FIDs throughout the excited volume:

$$S(t) = M_0 \int \rho(\mathbf{r})\,\mathrm{e}^{\,-\jmath\gamma\mathbf{r}\cdot\int_0^t \mathbf{G}(\tau)d\tau}\,d\mathbf{r}.$$

- Notice how the measured signal looks as if it's the **Fourier transform** of $\rho(\mathbf{r})$, the contrast-weighted density that is the desired image.
- If we rearrange the exponent of the exponential in terms of frequency space variables u and v, we can see how we can use the **inverse 2D FT to recover** $\rho(x, y)$.
- To image a 2D slice, we excite a slice of the imaged object at a particular location $z = z_0$. The RF coil signal from this slice is then:

$$S(t) = M_0 \iint \rho(x, y)\,\mathrm{e}^{\,-\jmath\gamma(x\,\mathbf{e}_x + y\,\mathbf{e}_y)\cdot\int_0^t \left[G_x(\tau)\,\mathbf{e}_x + G_y(\tau)\,\mathbf{e}_y \right] d\tau}\,dx\,dy.$$

The mathematical basis of 2D Fourier transform imaging

- Since $G_x(t)$ and $G_y(t)$ are adjustable linear gradients, we have full control of these. How can we manipulate these so as to sample the meaurement space on the desired grid?
- First, if we assume the **gradient fields are constant** throughout the period of their application, we may **replace the integrals** in the exponent of the exponential factor with the **pulse areas** giving:

$$\begin{aligned} S(t_x, T_y) &= M_0 \iint \rho(x, y)\,\mathrm{e}^{\,-\jmath\gamma(xG_x t_x + yG_y T_y)}\,dx\,dy \\ &= M_0 \iint \rho(x, y)\,\mathrm{e}^{\,-\jmath\gamma(xu + yv)}\,dx\,dy \end{aligned}$$

- If we **fix** G_x and **vary its period of application (the readout interval)** t_x, we can **sample horizontal frequency** u an arbitrary point in Fourier space using a single pulse sequence.
- If we **fix** G_y and **vary its period of application** T_y, we can **sample vertical frequency** v at an arbitrary point in Fourier space using a single pulse sequence.

The mathematical basis of 2D Fourier transform imaging

- For regular sampling, we could set $t_x = m\Delta t_x$ and $T_y = m\Delta T_y$ for the mth pulse sequence.
- However, since $S(t_x, T_y)$ is a **function of time**, the FID resulting from a **single pulse sequence automatically gives us all the values of $u = G_x\, t_x$ that we need.**
- Unfortunately, the 1D FID does not naturally evolve over T_y, so we must **artificially perturb** this "independent" variable.
- Consequently, if we have M rows of pixels, we must apply M pulse sequences so we can sample v at the M points that correspond to the y-locations of the pixel centers.
- Usually, it is desirable that the x and y gradient pulses have the same duration, and so normally G_y is varied rather than T_y. These two methods of sampling v are equivalent.

The mathematical basis of 2D Fourier transform imaging

- We can only apply a finite number of pulse sequences in practice, so the v-axis is sampled **discretely** as a function of T_y. Since $S(t_x, T_y)$ is the 2D FT of $\rho(x, y)$, we must sample along the y-axis of the image at a rate of $f_{sy} > \frac{2}{\Delta y}$, where Δy is the greater of the size of smallest feature in the image along the y-axis and the system resolution.
- Therefore M and ΔG_y must be chosen so that this sampling condition is satisfied.
- Since the FID is a **continuous** function of time, the u-axis will be continuous. In order to recover $\rho[n, m]$, we need to sample the FID in time so that the space domain constraint $f_{sx} > \frac{2}{\Delta x}$ is satisfied. Here Δx is the greater of the smallest feature in the image along the x-axis and the system resolution.
- The number of time samples N must be chosen so that this sampling condition is satisfied.

Image reconstruction in 2D Fourier transform MRI

1. The M RF signals are inserted as rows in a matrix according to the value of v to which they correspond.
2. The 2D inverse DFT is applied to the matrix.
3. This yields the reconstructed image.

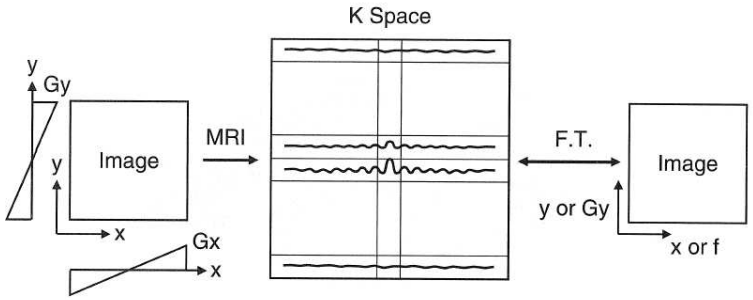

Figure 13-9. There is a one-to-one relationship between frequency and position along x axis and between phase-encode gradient increment and position along y direction.

Source: Hashemi p. 143

Image reconstruction in 2D Fourier transform MRI

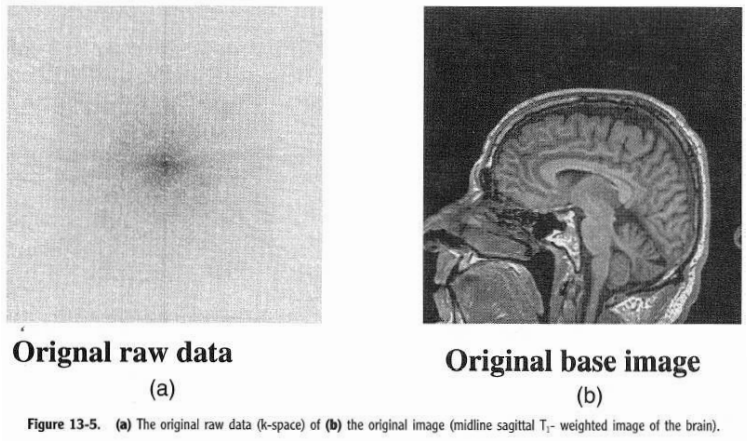

Figure 13-5. **(a)** The original raw data (k-space) of **(b)** the original image (midline sagittal T_1- weighted image of the brain).

Source: Hashemi p. 141

The left image shows the DC-centered 2D DFT that is constructed by inserting the RF FID signals as rows of the matrix. Applying the IDFT yields the original contrast distribution.

MRI frontiers: high field human imaging

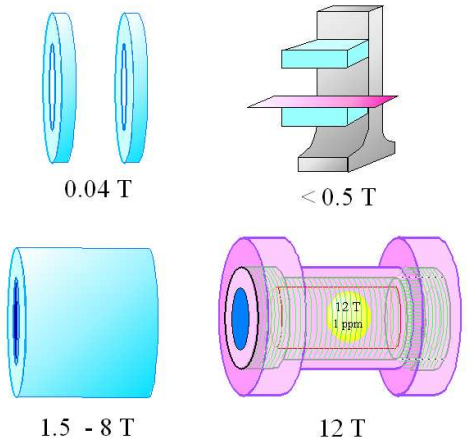

Over the last 25 years, MRI main field flux densities have increased from 0.04T to 8T. The next frontier is 12T.

MRI frontiers: high field human imaging

Why do we need high field?

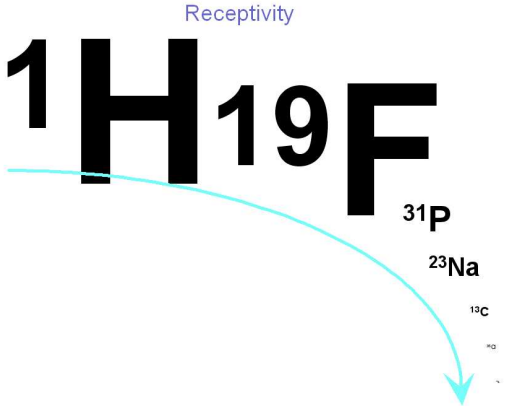

1. To image the molecular environments of nuclei other than protons. More complicated nuclei produce far smaller resonant signals. We need higher SNR.

MRI frontiers: high field human imaging

2. **SNR can be significantly improved** through use of high B_0. In NMR we have:

$$\text{SNR} \propto \gamma V B_0 \sqrt{t}$$

where V is the excited volume. To achieve a given SNR, a study at 12T that takes $t = 5$ minutes would take 5 hours at 1.5T on a current clinical scanner.

3. The **frequency separation** between the **spectral lines** of different molecular species is **greater at higher field strengths**. This improves MRS resolution.

Problem: A high uniform field is very difficult to create in a magnet with a large bore. Until recently, no materials were available that can achieve this field strength in an electromagnet.

MRI frontiers: high field human imaging

Previously, the best known alloy was one of niobium and titanium. Fields in excess of 10T are very difficult to achieve at reasonable cost using this material.

Enabling Technology: Nb_3Sn Superconductors

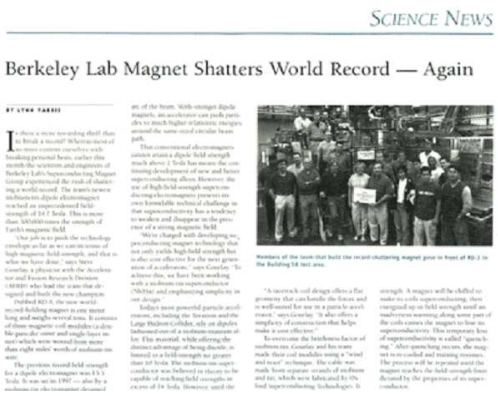

SCIENCE NEWS

Berkeley Lab Magnet Shatters World Record — Again

MRI frontiers: high field human imaging

An alloy of niobium and tin was used to create the most powerful dipole electromagnet in the world producing a flux density of 14.7 T. For a 12T magnet, approximately 10 times the amount of NbTi wire is required than for Nb_3Sn.

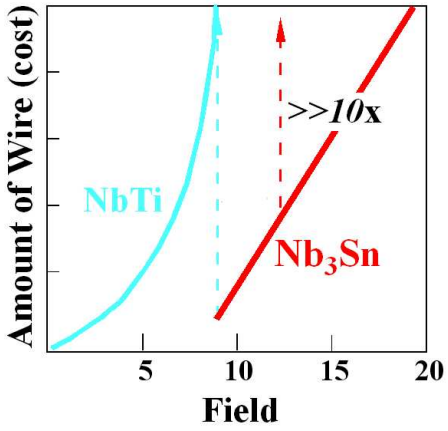

MRI frontiers: high field human imaging

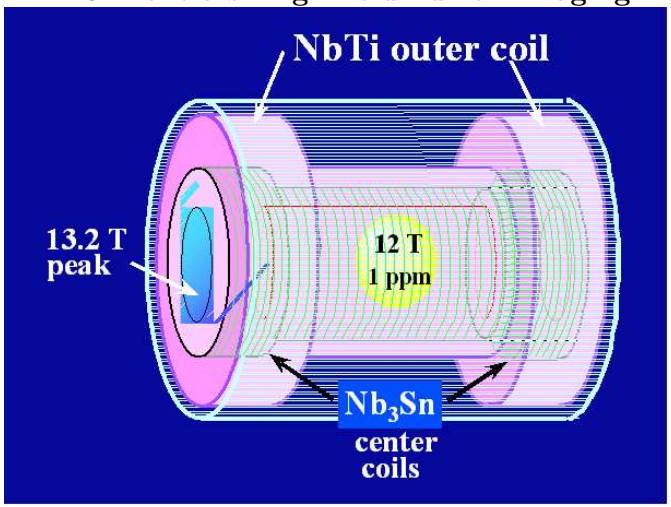

Conceptual design of a 12T magnet for human imaging. It calls for a central field "sweet spot" where field inhomogenieties are less than 1 part per million of the field strength.

MRI frontiers: high field human imaging

What studies would be enabled by a 12T magnet?

Human Noninvasive Studies Enabled by 12 T

Examples

Cellular and extracellular concentrations of Na, K, Cl with relevance to mental disorders, hypertension and cancer

Role of the pentose monophosphate shunt in cancer, congestive heart failure and ischemic heart disease

Glutamate / Glutamine metabolism in the normal CNS and in stroke and trauma

Amyloid plaque concentration changes on the CNS in neurodegenerative disorders

Carbohydrate and fatty acid metabolism in obesity and nutrition

CNS ≡ central nervous system

MRI frontiers: high field human imaging

Example *in vitro* animal study:

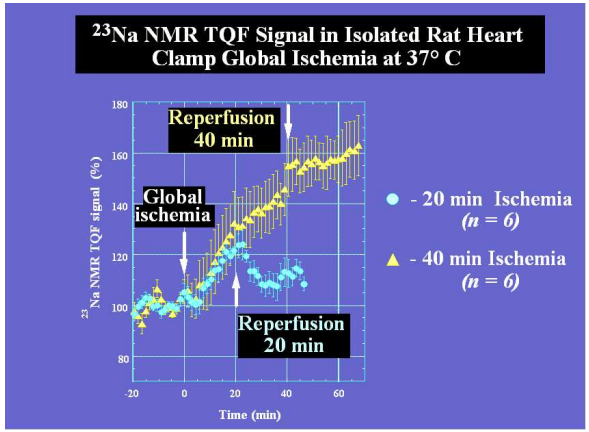

In this example, NMR spectroscopy is performed at high field on a rat heart. When blood supply is clamped, ischemia ensues. During ischemia, the intracelluar Na concentration increases. If flow is restored after 20 minutes, the intracellular Na level goes back down. After 40 minutes of blood flow occlusion, the Na level does not decrease, suggesting that irreversible cellular damage has occurred.

Comparison of MRI, x-ray CT and ECT

Modality:	**MRI**	**x-ray CT**	**ECT**
Contrast agent	optional	optional	required
Minimum detectable tracer concentration	10^{-6}	N/A	10^{-8} (PET)
Functional contrast	limited	limited	excellent
Max. resolution	sub-mm	sub-mm	≈ 1 mm (PET). theoretically unlimited, typ. 5 mm (SPECT)
Soft tissue contrast	excellent	poor	N/A
Bone imaging	marrow visible bone invisible	excellent	bone metabolism
Ionizing radiation dose	none	significant esp. for 3D scan	significant
Slice scan time	sec.-min.	seconds	minutes
Audio noise & patient isolation	80-90 dB, significant	minimal	minimal
Pacemakers, implants, claustophobia	excludes subject	implants cause local artifacts	implants cause local artifacts

Comparison of MRI, x-ray CT and ECT

Modality:	**MRI**	**x-ray CT**	**ECT**
Complexity	very high	low	low-moderate
Spectroscopy	possible	impossible	impossible
Flow measurement	good	limited	fair
Timing resolution	good	good	poor
Tissue heating	significant esp. @ high B_0	negligible	negligible
Equipment cost (order of magn.)	$\$10^6+$	$\$10^5+$	$\$10^5+$ (SPECT) $\$10^6+$ (PET)
Maintenance costs	very high	moderate	high (PET) moderate (SPECT)
Cyclotron required	no	no	generally (PET)
Supercooling	required	no	not generally
Worldwide deployment (order of magn.)	10^4	10^5	10^5 (SPECT) 10^2 (PET)